Influence of MJO on Asian Climate and its Performance of JMA Monthly Forecast Model

Satoko Matsueda, Yuhei Takaya and Kengo Miyaoka
Climate Prediction Division, Japan Meteorological Agency

Madden—Julian Oscillation (MJO)

- The MJO is the dominant mode of intraseasonal variability in the tropics.
- The MJO influences not only the tropical weather and climate but also the extratropical circulations.

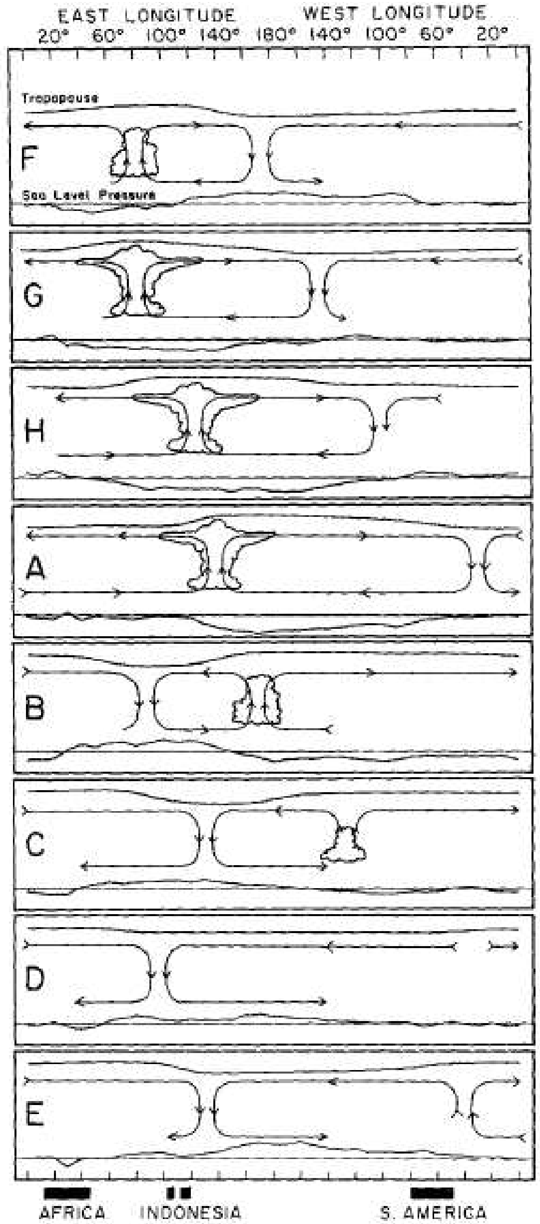

Madden and Julian (1994)

Influence of MJO on Global circulation

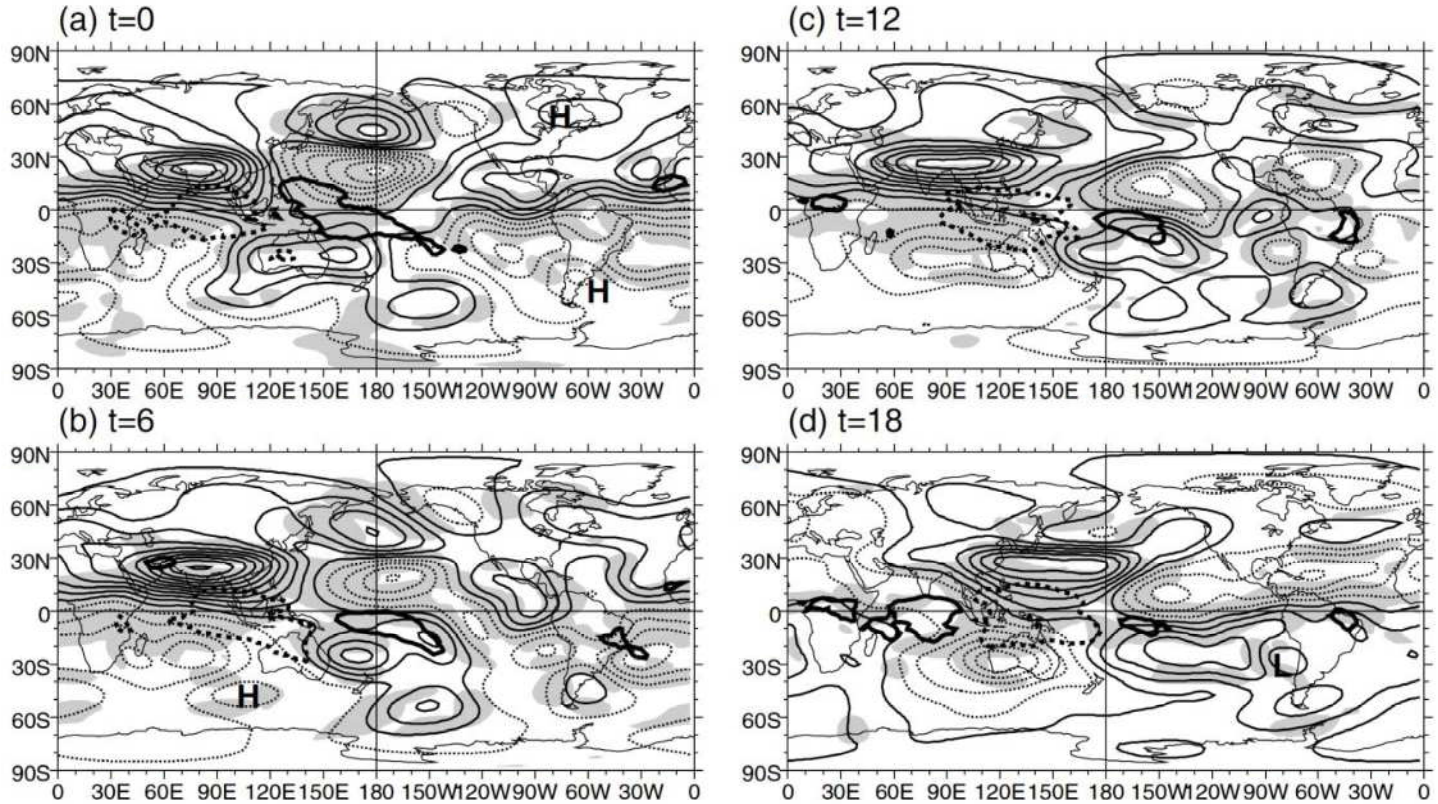

Figure 1. Regression maps of outgoing long-wave radiation (OLR) and 200 hPa stream function at 6-day intervals during the first half of the MJO cycle, scaled to a deviation of PC1/2 = 2.0. OLR is contoured heavily at -10 W m^{-2} (dotted) and 10 W m^{-2} (solid). Stream function contour interval is 1.25×10^6 m^{2}s^{-2}, with negative contours dotted. For clarity, the H and L symbols indicate selected local stream-function maxima and minima, respectively. Regions are shaded where either the u or v component of the 200 hPa wind is locally significant at the 95% level.

Regression maps of OLR and ψ200

MJO has a statistically significant upper-tropospheric equatorial wave patterns linked to the tropical convection anomalies, and extratoropical wave patterns.

Matthews et al. (1994)

Influence of MJO on Asian Climate

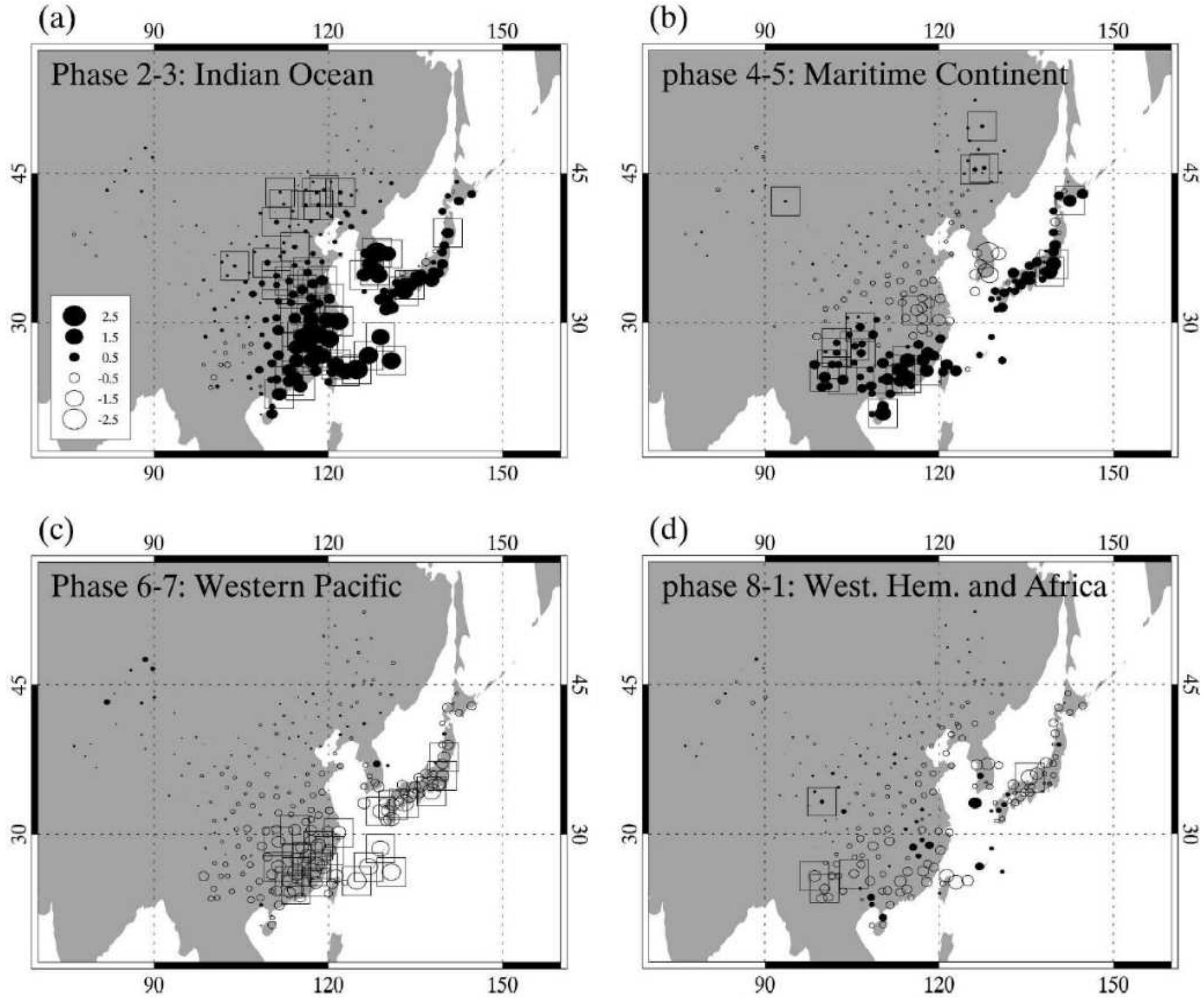

FIG. 2. Average precipitation rates (mm day^{-1}) in each of the categorized MJO phases, represented as differences from the winter-mean values. Squares indicate the stations where the composite values are significant at the 99% confidence level.

In phase 2-3
(the MJO-related convection center is located around the Indian Ocean), the precipitation increases considerably in most parts of the East Asian region.

In phase 6-7, the precipitation decreases over the region from southeast China to Japan.

Jeong et al. (2008)

Influence of MJO on Asian Climate

Composite : initial Phase 2 (active convection in Indian Ocean)

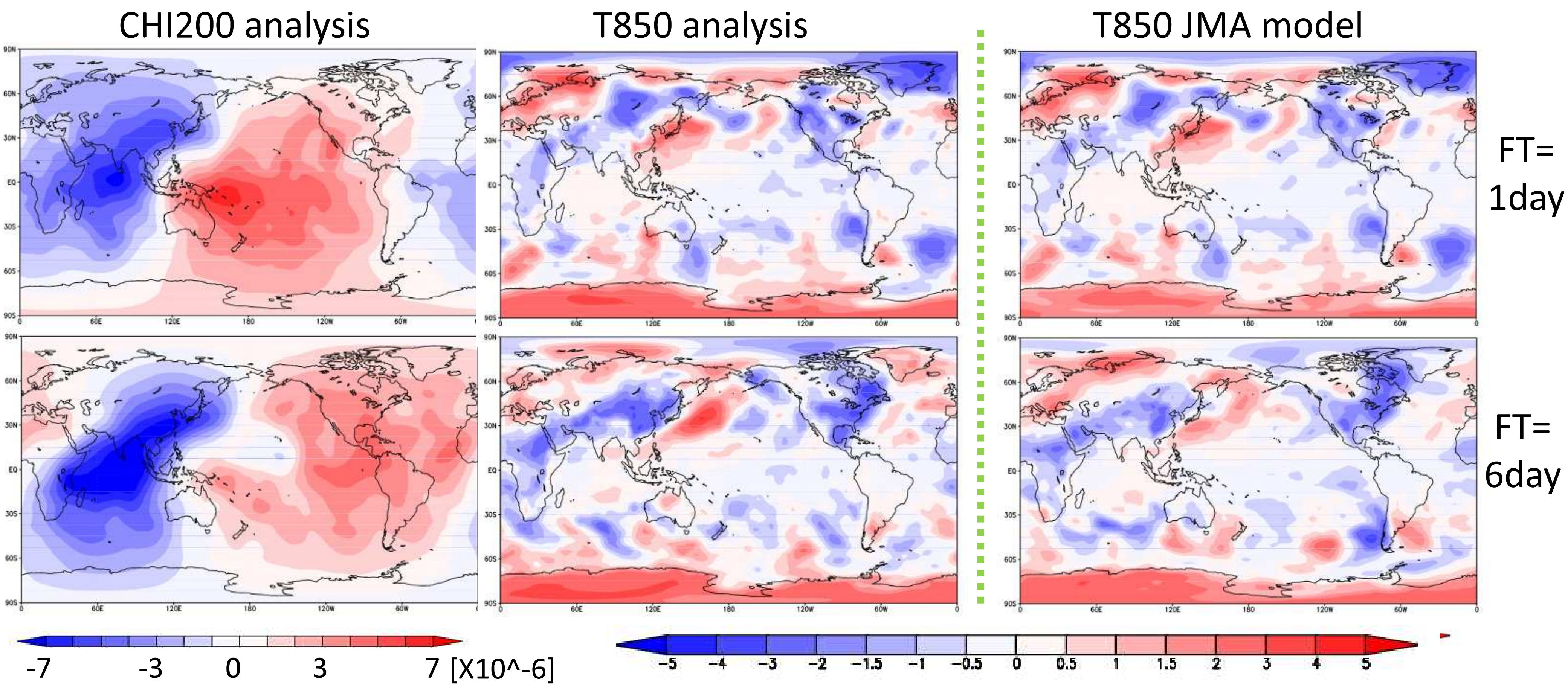

When active convection is in Indian Ocean, T850 anomaly pattern can be reproduced in Asia.

- The MJO forecast performance of the JMA operational monthly forecast model is examined.
- We use a diagnostic package developed by the U.S. Climate Variability and Predictability (CLIVAR) MJO Working Group (CLIVAR Madden-Julian Oscillation Working Group 2009).

Data

- Analysis data (daily, 2.5° × 2.5°)
  - U, V, T, Q, CHI : JRA-25 (1979-2001)
  - OLR : NOAA (1979-2001)
  - Precipitation : GPCP (1997-2008)

- Hindcast data by JMA monthly model

Resolution	TL159L60 (～110km)
Initial time	10th , 20th and the end of each month
Forecast length	40 days
Ensemble size	5
SST	Initial anomaly persistence
Period	1979-2001

CEOF for observations

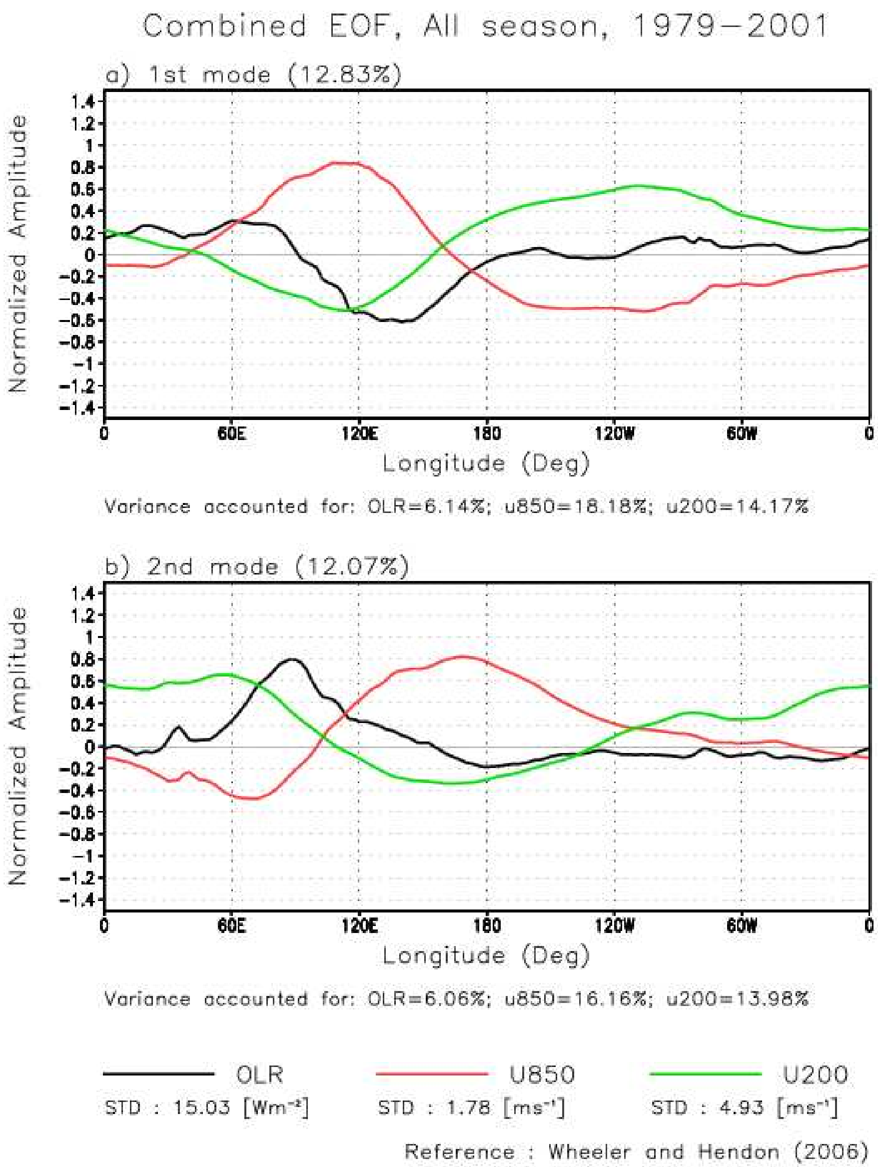

Power spectra of projected PC1

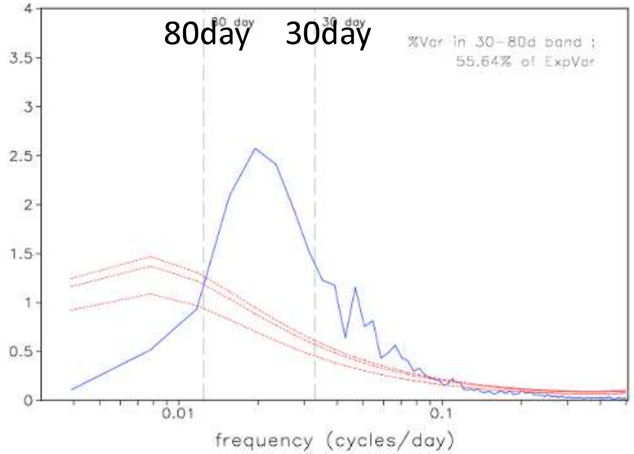

Power spectra of projected PC2

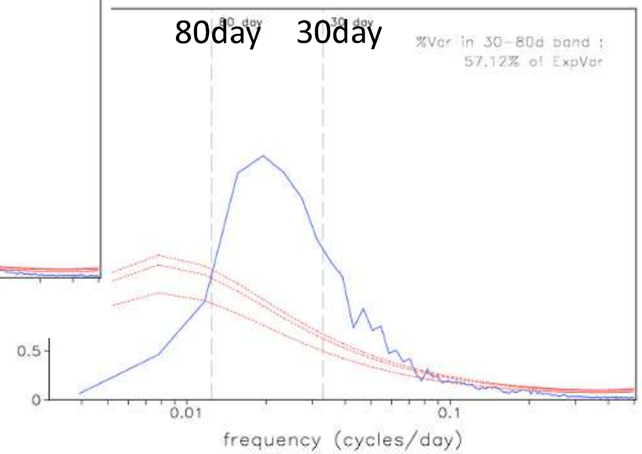

Combined EOF analysis is conducted for daily fields of equatorially-averaged (15S to 15N) OLR, U850, and U200 for the period of 1979 to 2001 (23 years). Before the EOF analysis,

- remove the long-term (23-year) mean from each field at each grid point.
- remove a 120-day mean of the most recent 120 days at each point.
- normalize each field by the square-root of its global mean variance.

Wheeler and Hendon (2004)

MJO diagram

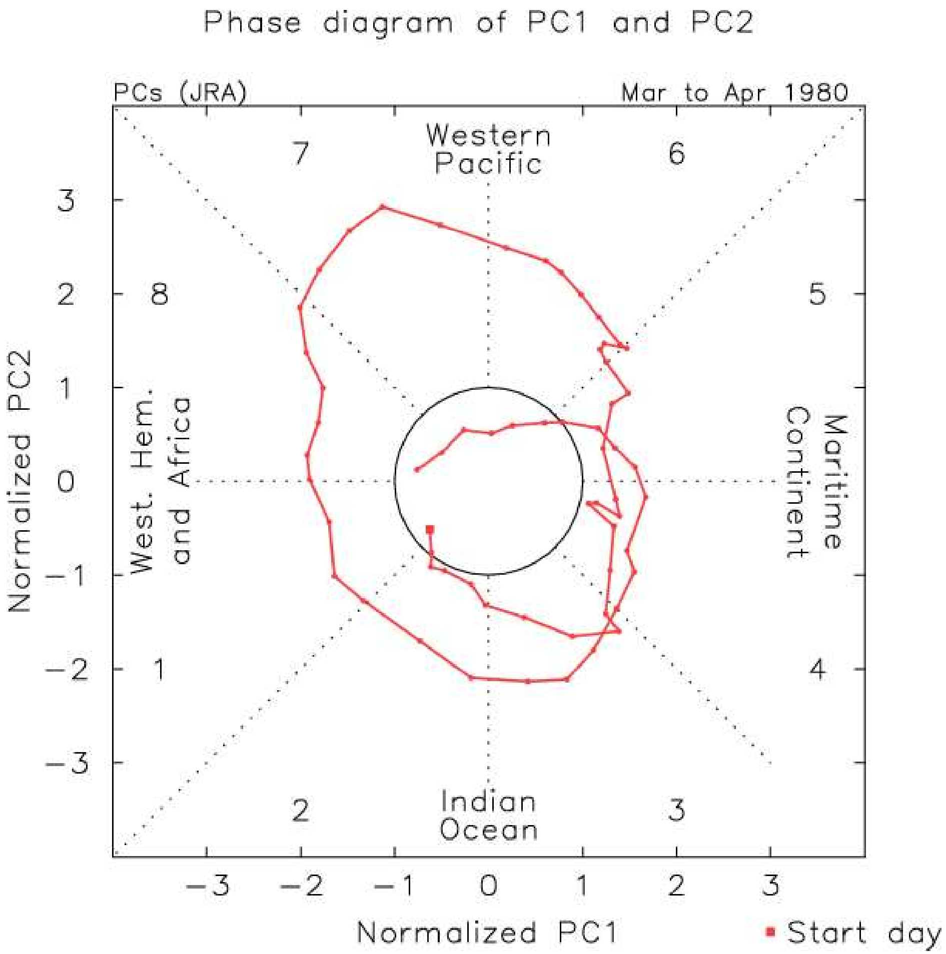

Fig. Phase diagram of Normalized PC1 and PC2
(01Mar1980 to 30Apr1980)

PC1 and PC2 are the x axis and y axis, respectively. The numbers within each octant (from 1 to 8) are the defined MJO phase, and the words on each side of the diagram describe the approximate location of MJO associated convection along the equator.

MJO index skill

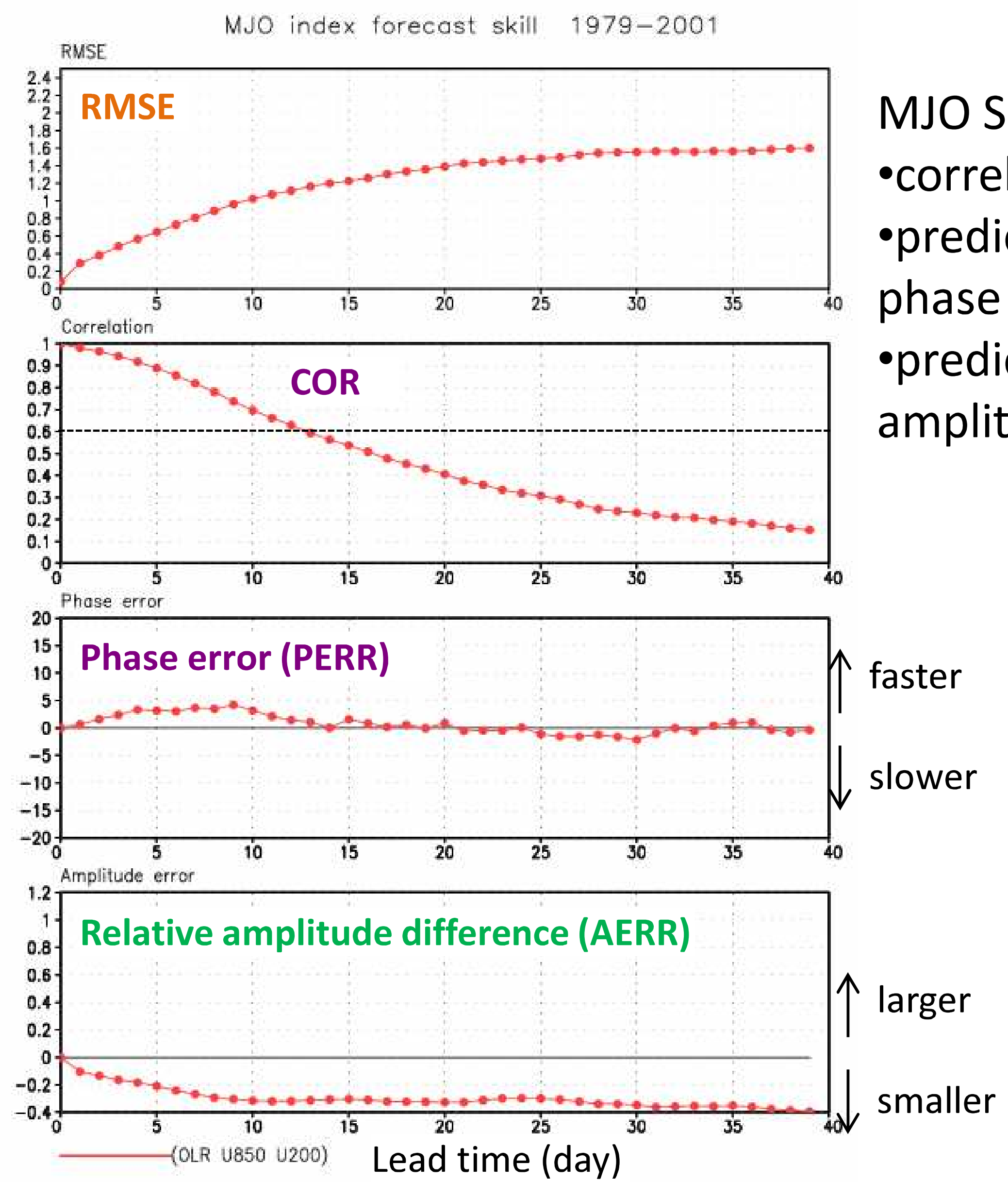

MJO Skill of JMA monthly models

- •correlation coefficient falls below 0.6 on day 13
- •predicted phase speed is faster than observed phase speed
- •predicted amplitude is smaller than observed amplitude

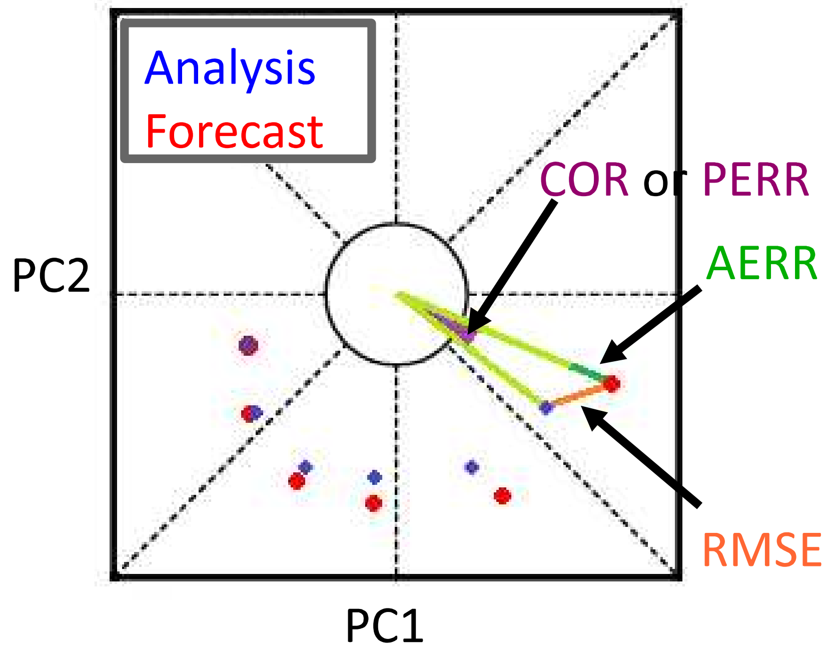

MJO index composite

analysis model

Summer

Winter

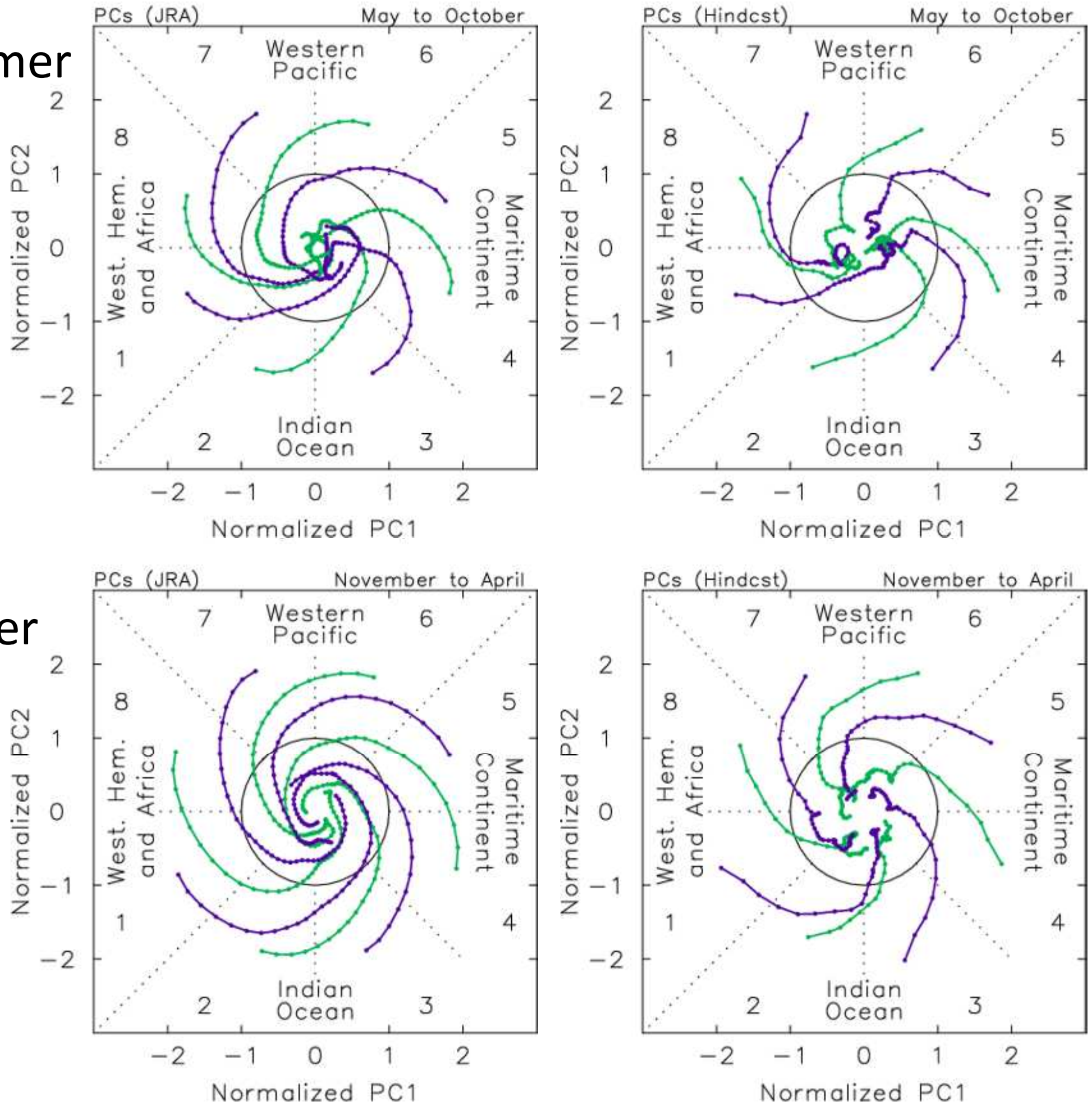

Table days with the MJO amplitude of > 1.0

Initial phase		1	2	3	4	5	6	7	8
Summer	Analysis	10	9	12	13	10	12	16	12
	Model	7	10	9	8	9	7	11	8
Winter	Analysis	19	15	13	14	17	15	14	15
	Model	11	9	8	7	14	11	7	7

Simulated active MJO period (amp. >1.0) is almost shorter than observed one.

Fig. composite of (left) observed and (right) simulated PC1 and PC2 from each initial MJO phase with amplitude of > 1.5 during (top) summer and (bottom) winter

Hovmöller composite Precipitation Winter

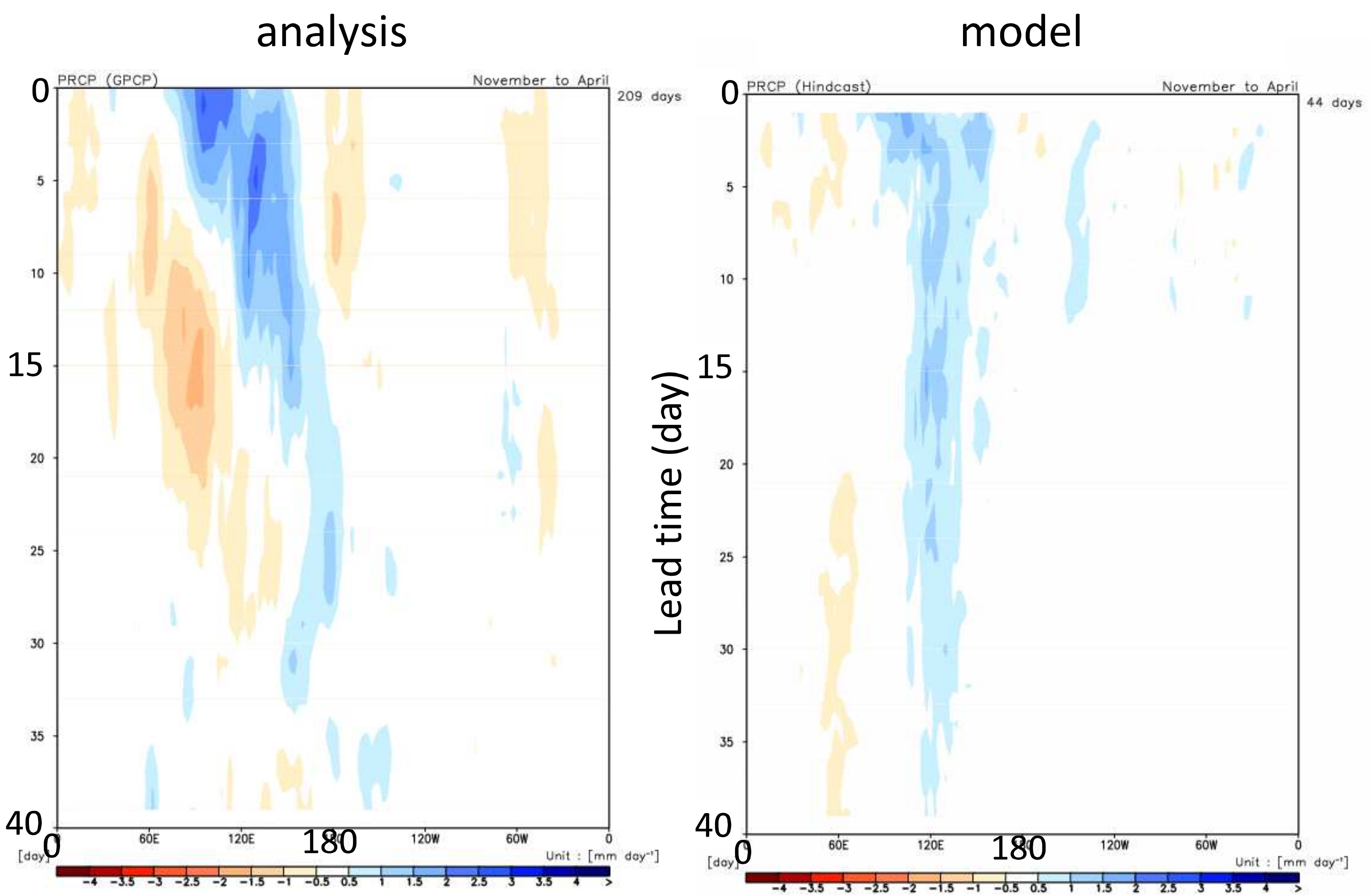

Initial phase 3 (active convection in Eastern Indian ocean)

Eastward propagation is not simulated by the model.

Fig. Composite of equatorially-averaged (15S-15N) precipitation for analyses(left) and hindcast(right) started from phase 3 with the initial amplitude of > 1 σ

Hovmöller composite CHI200 Winter

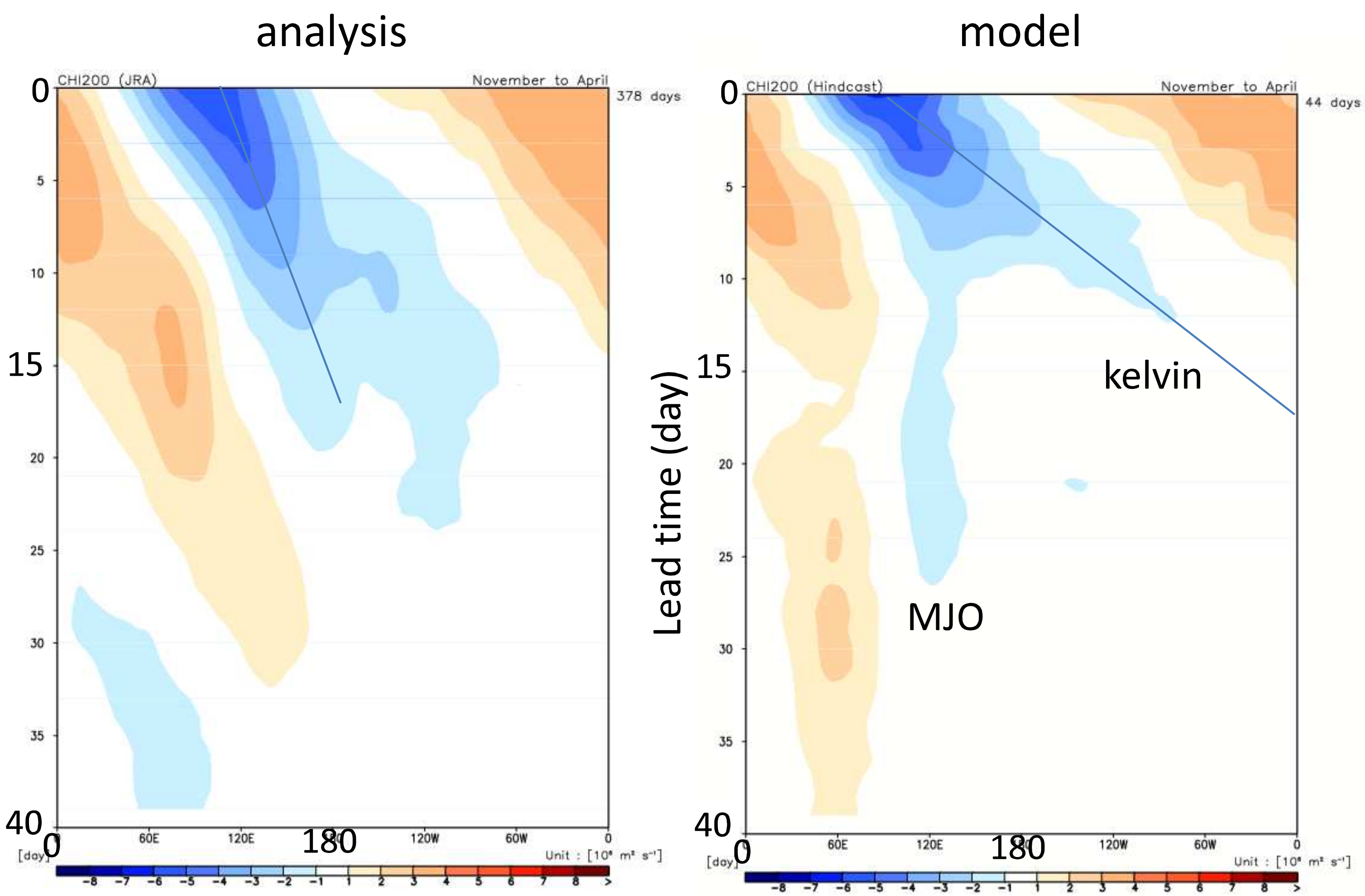

Fig. Composite of equatorially-averaged (15S-15N) CHI200 for (left) analyses and (right) hindcast started from phase 3 with the initial amplitude of > 1 σ

Initial phase 3 (active convection in Eastern Indian ocean)

Eastward propagation is well simulated by the model up to a lead time of 10 days.

The model simulates Kelvin waves that have faster phase speed and the MJO that do not propagate eastward.

Lag-Longitude diagram OLR/U850 Winter

analysis

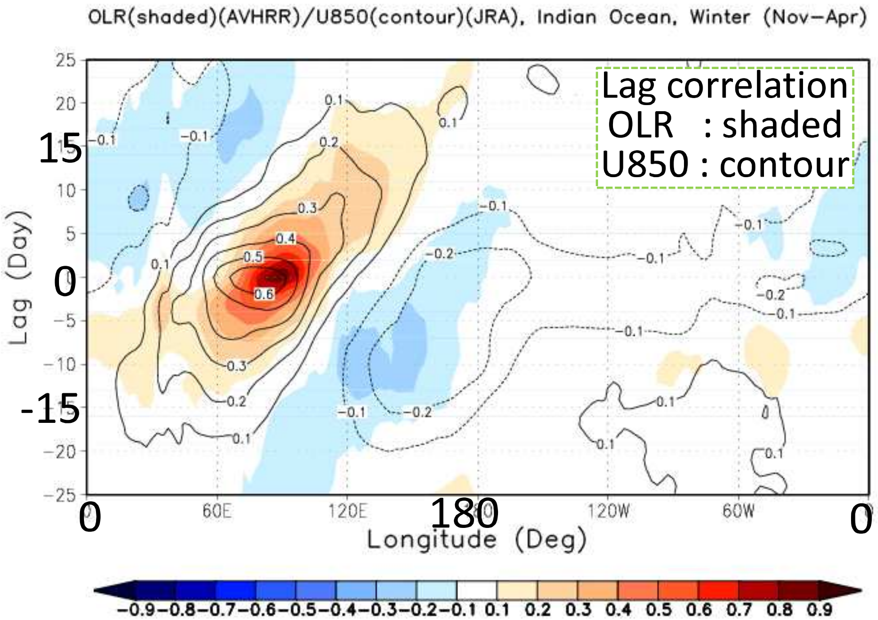

model (FT=10day : lag=0)

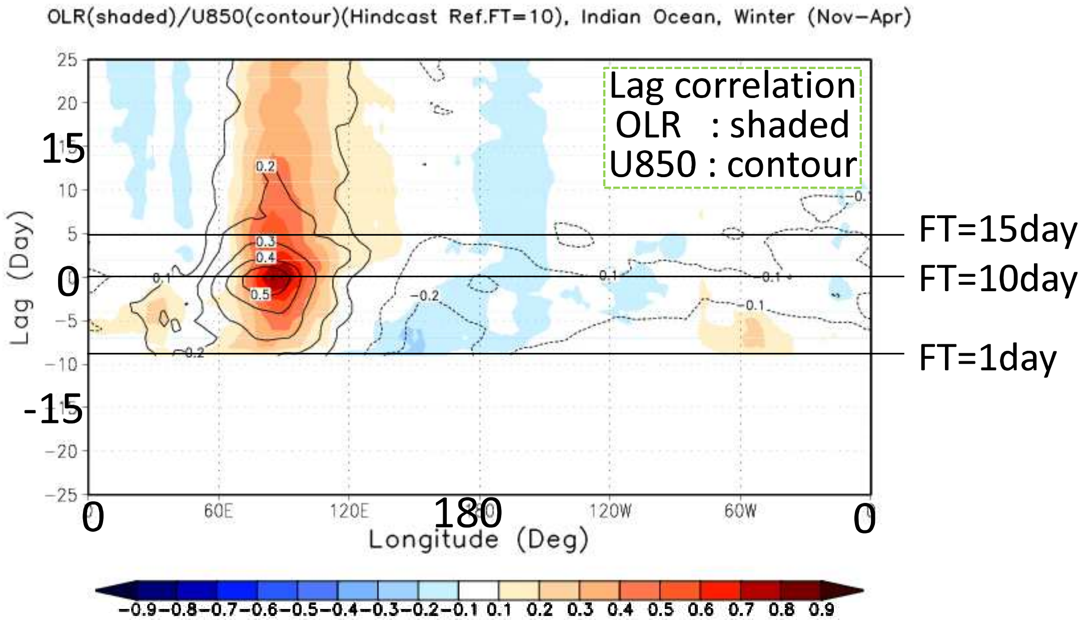

Eastward propagation of OLR/U850 anomaly is not simulated.

Fig. Lag correlation of intraseasonal OLR(shaded) and U850(contour) averaging 10S-10N at all longitudes against OLR and U850 at an Indian Ocean reference point (OLR:10S-5N,75-100E, U850:1.25-16.25S,68.75-96.25E).

For hindcast, a forecast time of 10day corresponds lag = 0.

Lag-Latitude diagram OLR/U850 Summer

analysis

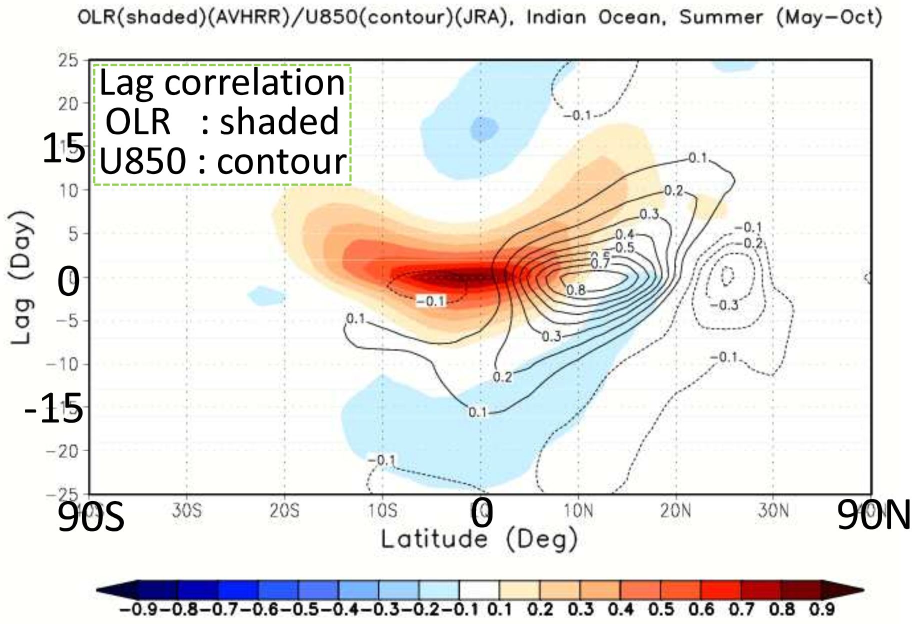

model (FT=10day : lag=0)

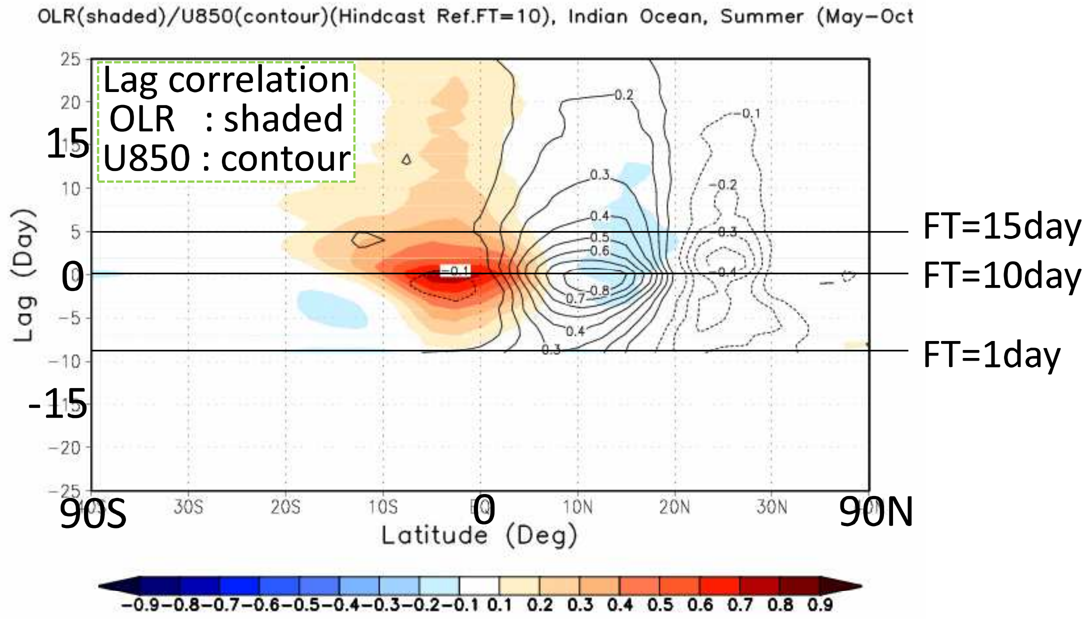

Northward propagation of OLR/U850 anomaly in Indian Ocean in summer is not simulated.

Fig. Lag correlation of intraseasonal OLR(shaded) and U850(contour) averaging 80-100E at all latitudes against OLR and U850 at an Indian Ocean reference point (OLR:10S-5N,75-100E, U850:3.75-21.25N,68.75-96.25E).

For hindcast, a forecast time of 10day corresponds lag = 0.

MJO Life cycle composite OLR/Wind200 Summer

analysis

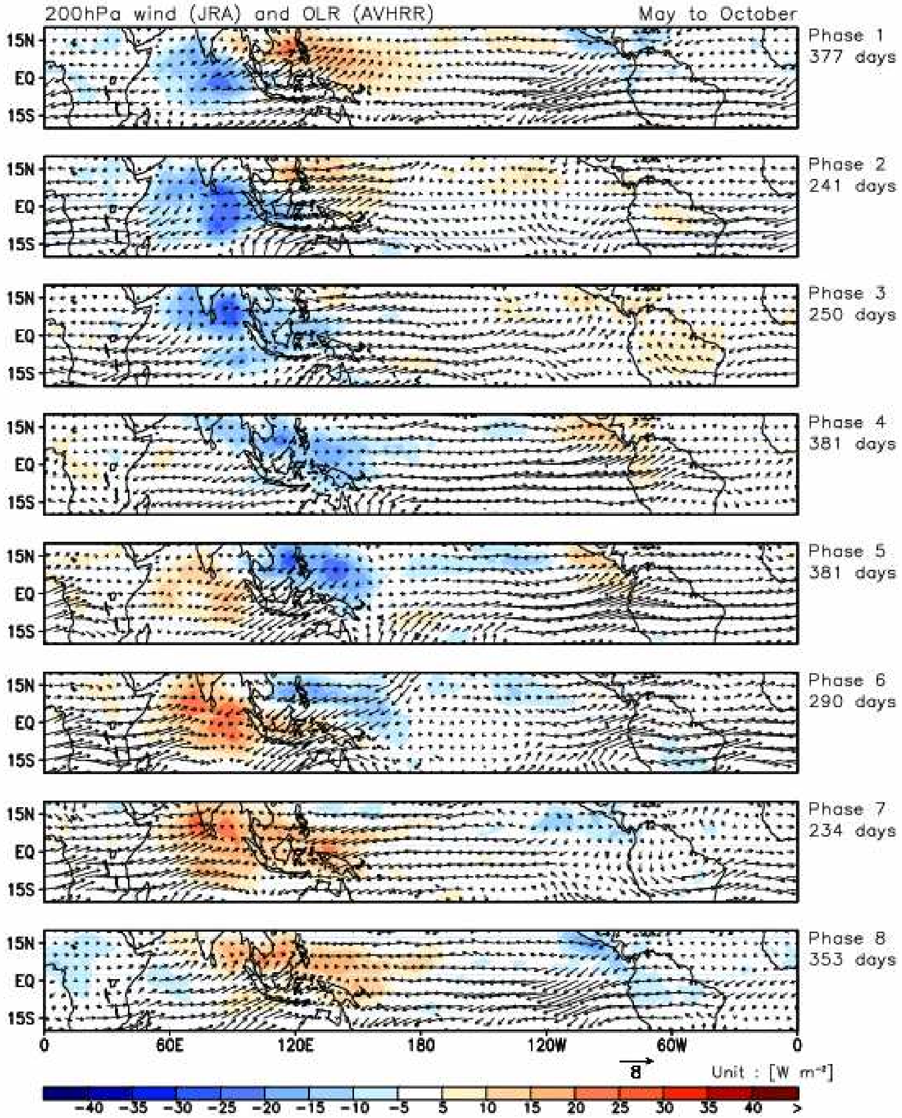

model FT=2week

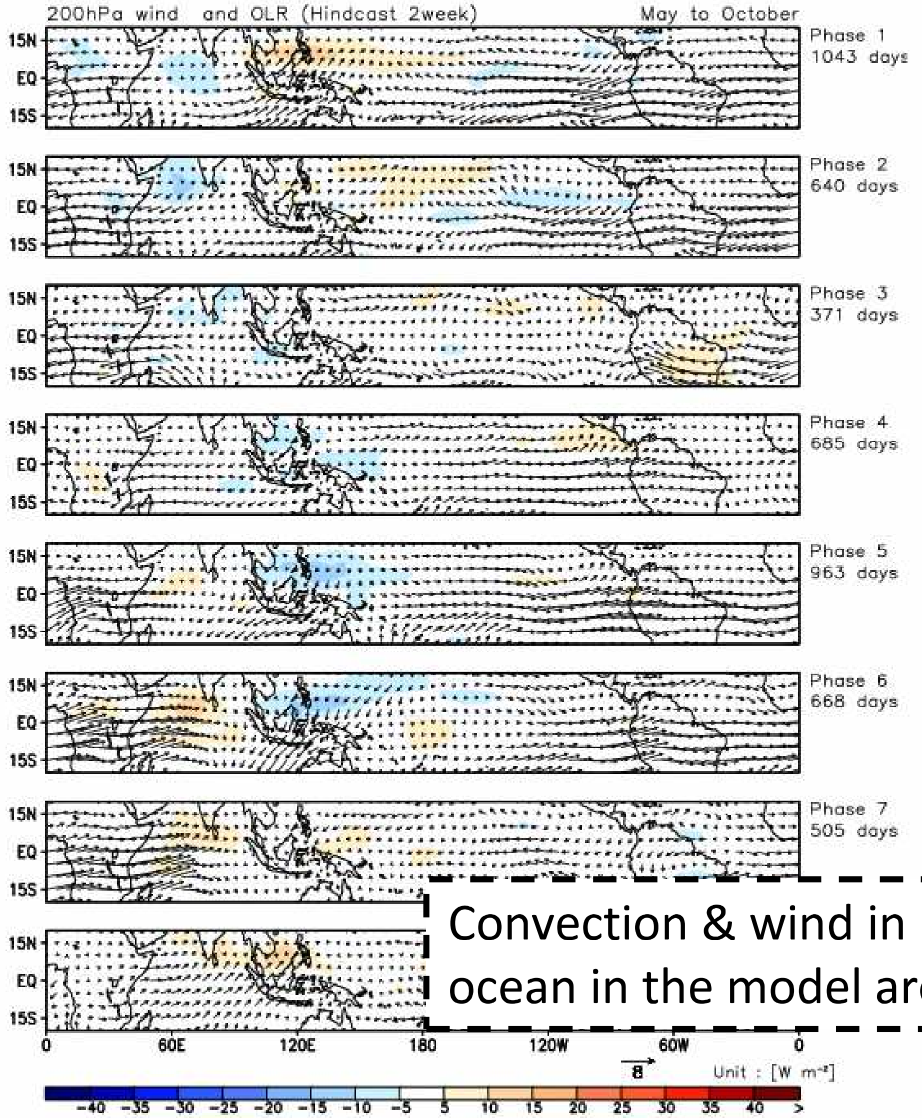

Convection & wind in Indian ocean in the model are weaker.

MJO Life cycle composite OLR/Wind200 Winter

analysis

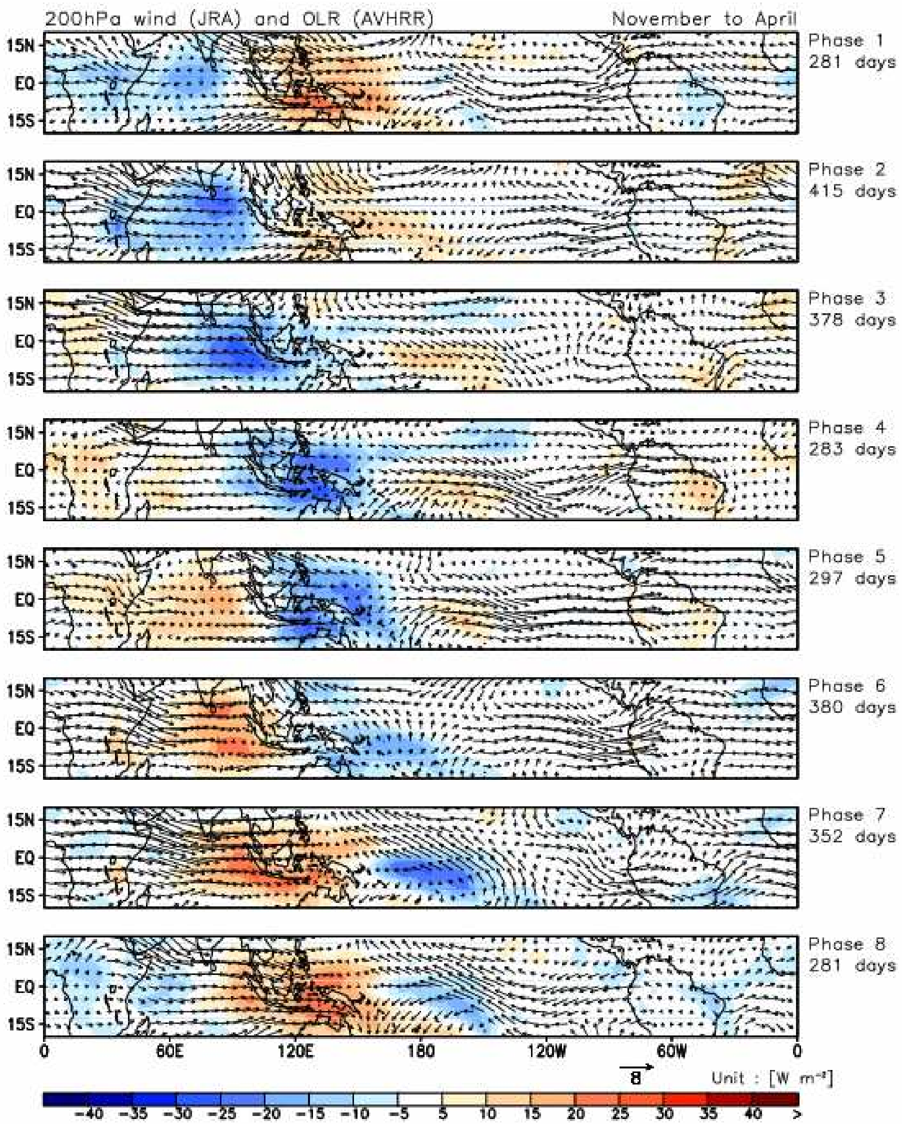

model FT=2week

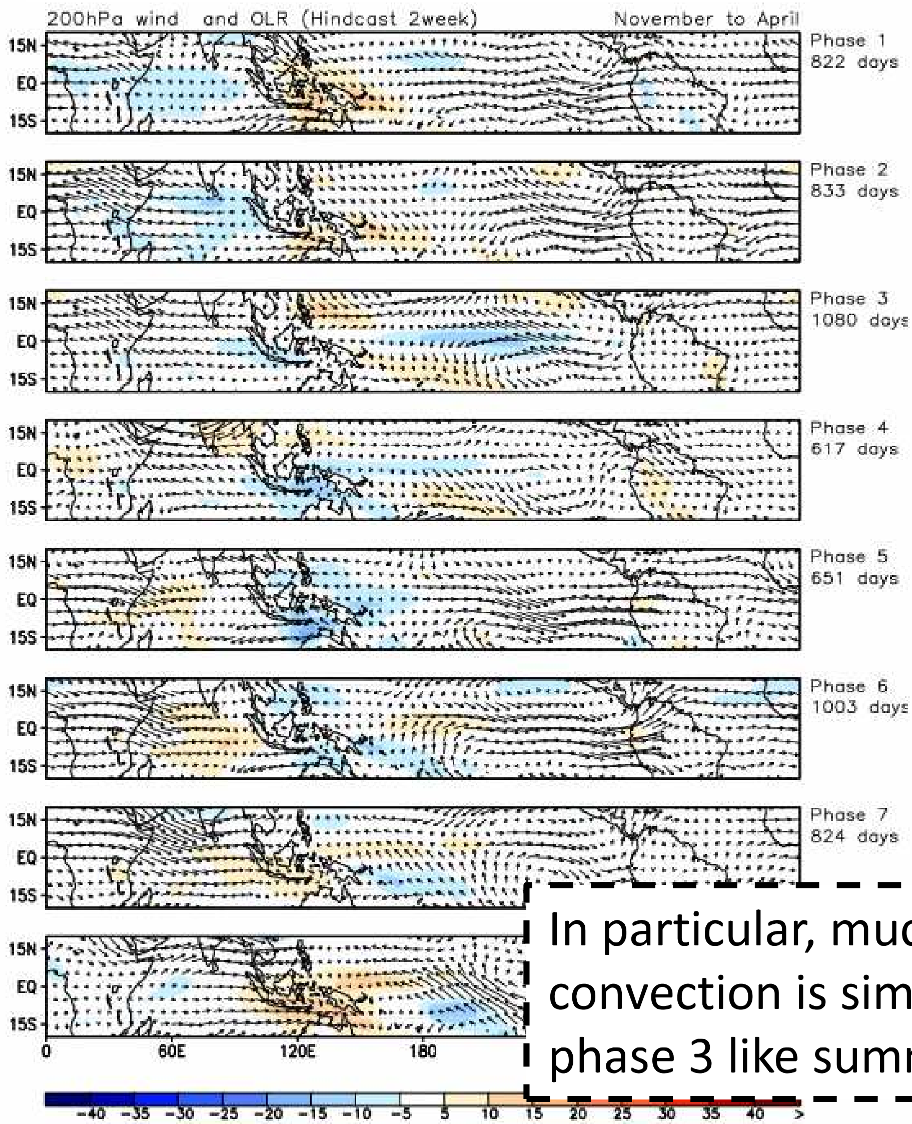

In particular, much weaker convection is simulated in phase 3 like summer.

Conclusions

- The MJO forecast performance is relatively good up to a lead time of 2 weeks. However, the predicted MJO phase speed is faster than observed phase speed, and the predicted MJO amplitude is smaller than observed amplitude.
- The eastward propagation of active convection (OLR/Precip) in the model is weaker than analysis.
- The model does not also well reproduce the northward propagation in the Indian Ocean in summer.
- In particular, much weaker convection than the analysis is simulated in Indian Ocean.
- It is necessary to further improve the model for more realistic representation of the MJO.

Backup Slides

MJO Life cycle composite T/Q(vertical structure)

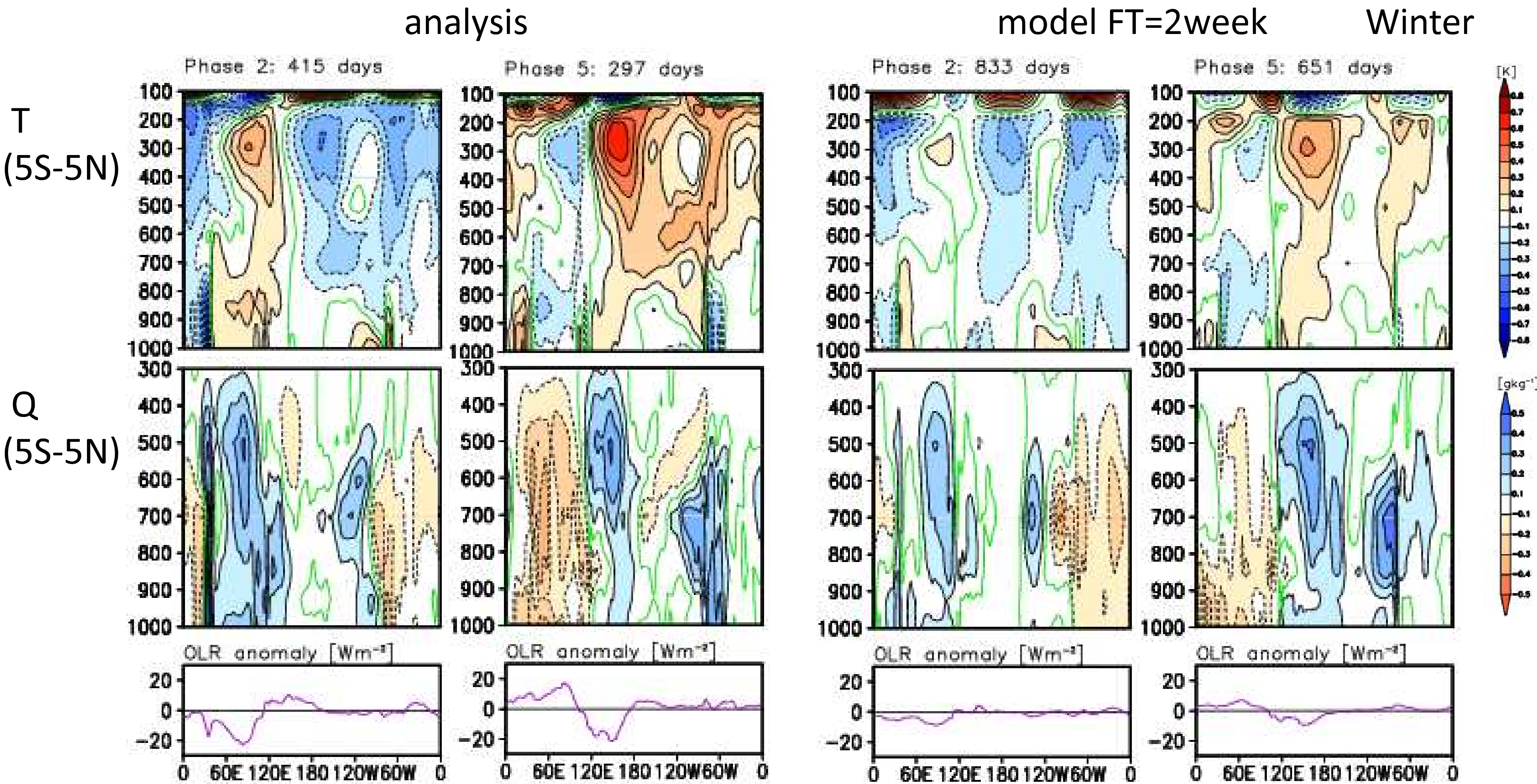

Simulated vertical heating is not enough in active convection.

MJO Life cycle composite T(vertical structure)

analysis

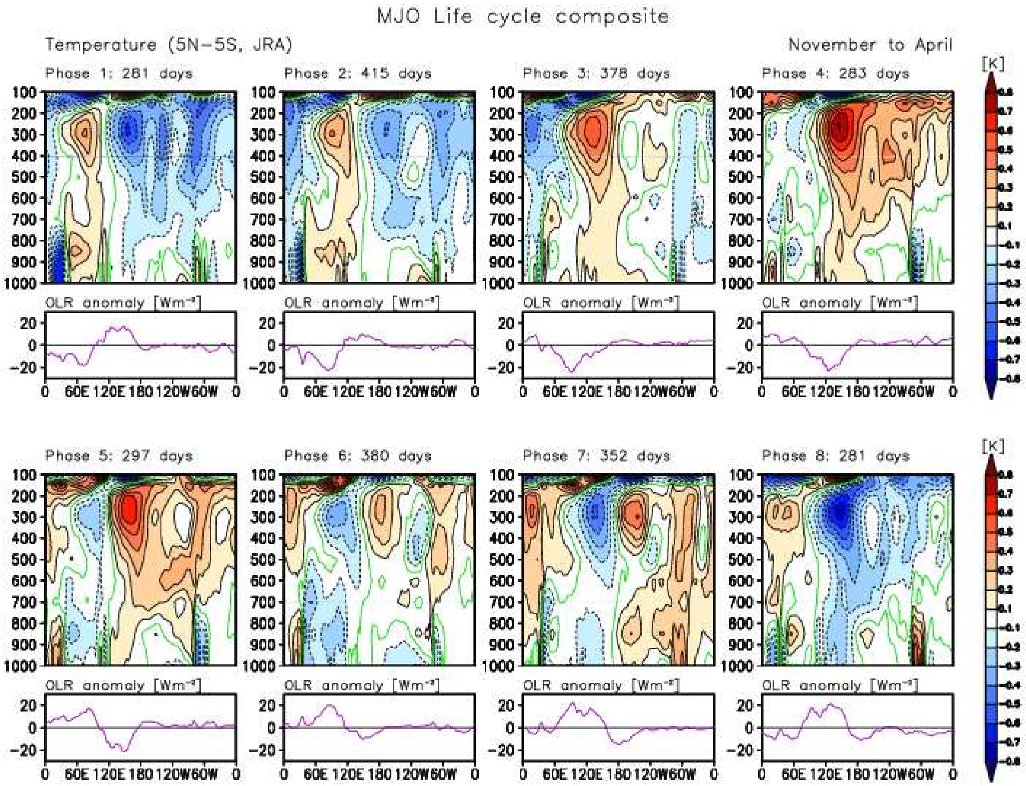

model FT=2week

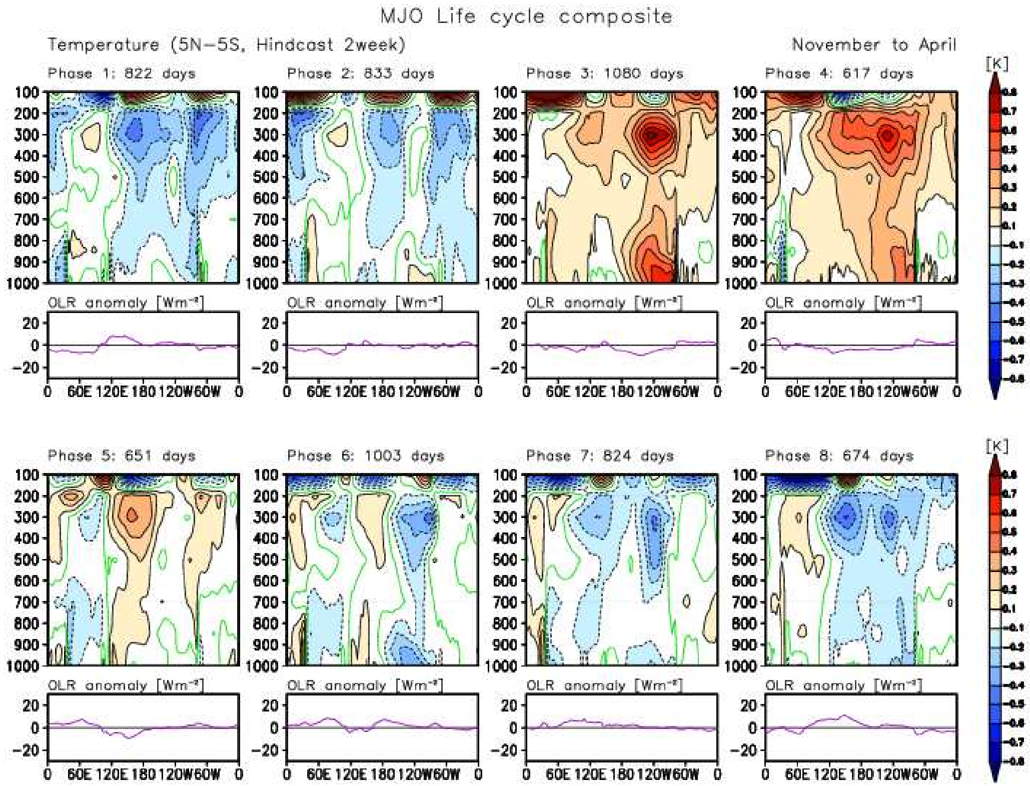

MJO Life cycle composite Q(vertical structure)

analysis

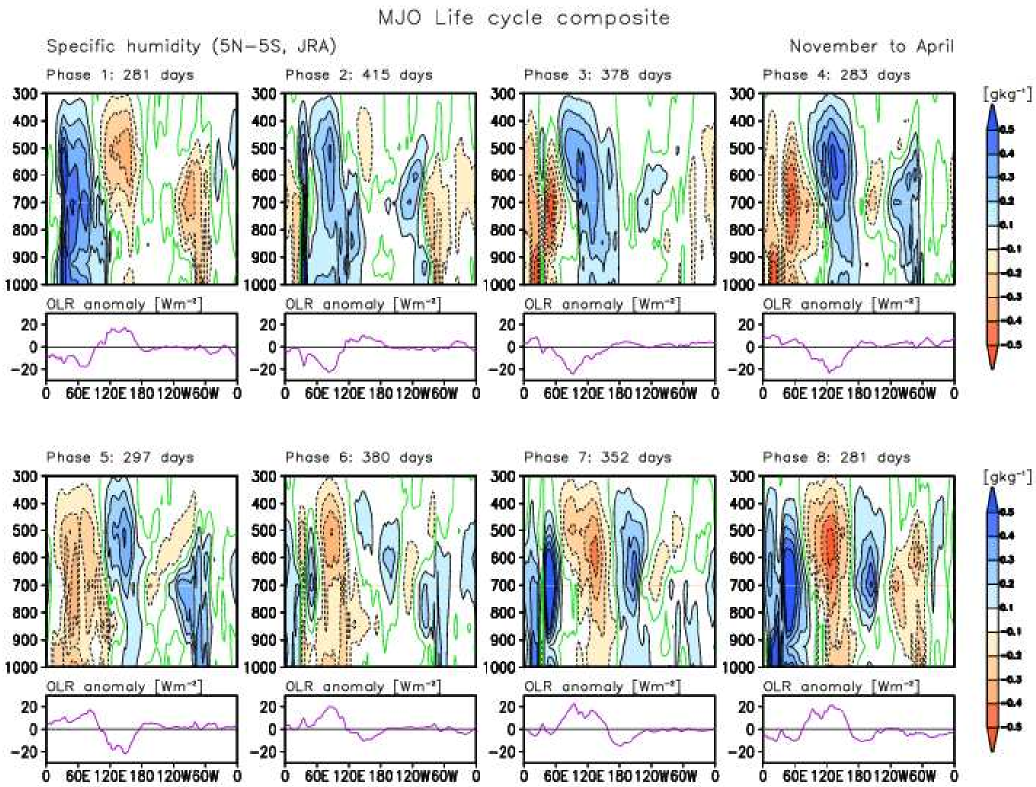

model FT=2week

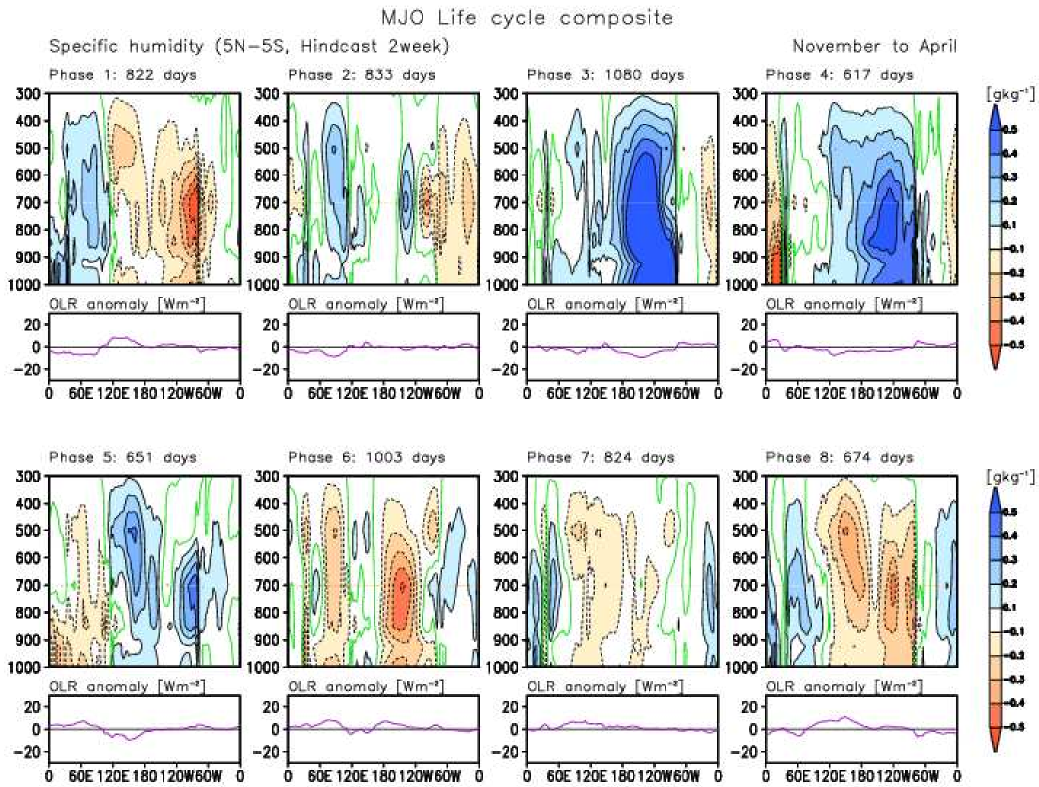

MJO index skill

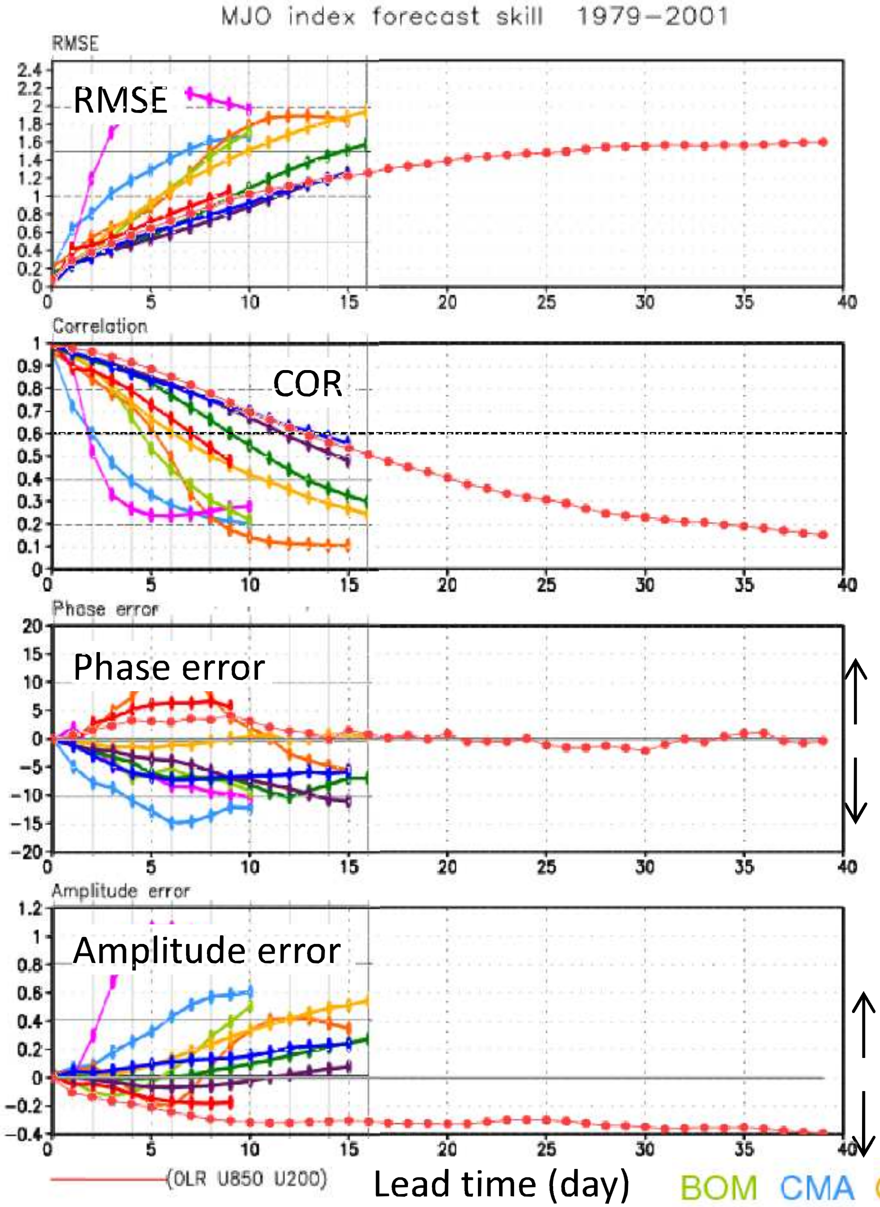

MJO Skill of JMA monthly models

- •correlation coefficient falls below 0.6 on day 13
- •predicted phase speed is faster than observed phase speed
- •predicted amplitude is smaller than observed amplitude

$$\mathrm{RMSE}(\tau) = \sqrt{\frac{1}{N}\sum_{t=1}^{N}\left(\left(f_1(t,\tau) - a_1(t)\right)^2 + \left(f_2(t,\tau) - a_2(t)\right)^2\right)}$$

$$\mathrm{COR}(\tau) = \frac{\sum_{t=1}^{N}\left(a_1(t)f_1(t,\tau) + a_2(t)f_2(t,\tau)\right)}{\sqrt{\sum_{t=1}^{N}\left(a_1(t)^2 + a_2(t)^2\right)}\sqrt{\sum_{t=1}^{N}\left(f_1(t,\tau)^2 + f_2(t,\tau)^2\right)}}$$

$$\mathrm{PERR}(\tau) = \frac{1}{N}\sum_{t=1}^{N}\tan^{-1}\left(\frac{a_1(t)f_2(t,\tau) - a_2(t)f_1(t,\tau)}{a_1(t)f_1(t,\tau) + a_2(t)f_2(t,\tau)}\right)$$

$$\mathrm{AERR}(\tau) = \frac{1}{N}\sum_{t=1}^{N}\left(\sqrt{f_1(t,\tau)^2 + f_2(t,\tau)^2} - \sqrt{a_1(t)^2 + a_2(t)^2}\right)$$

Matsueda and Endo (2011)

気象庁1か月予報モデルで再現される熱帯波動の特徴（AMIPラン）

- Wheeler and Kiladis (1999)の手法による時空間スペクトル解析（対流結合した赤道波分散関係）

降水量（観測 GPCP-1DD）

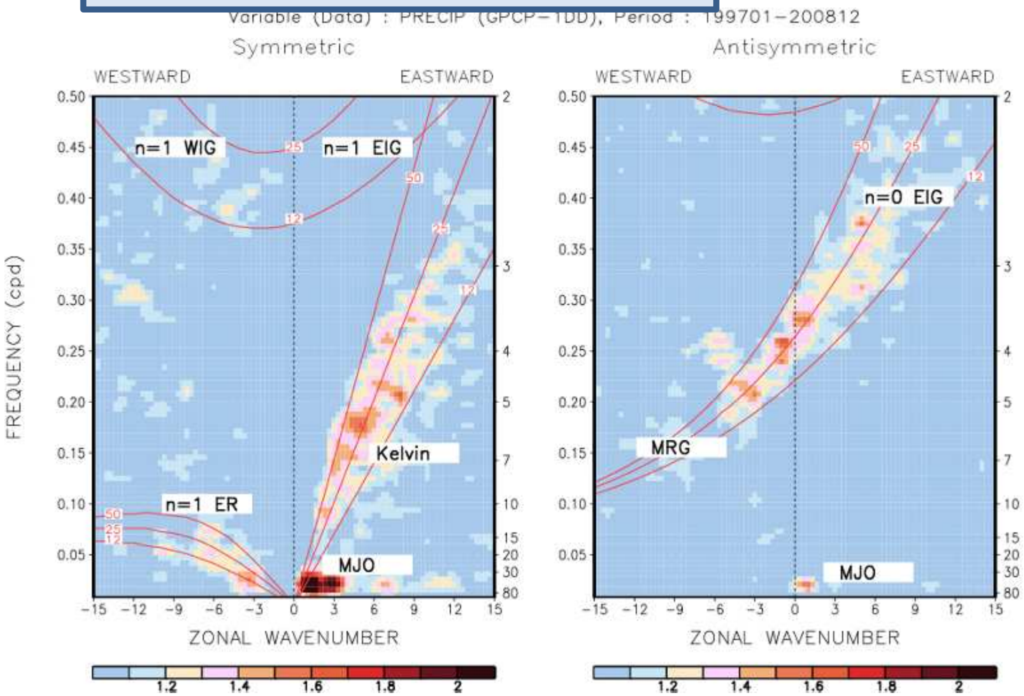

GSM1103C (1980-2010)

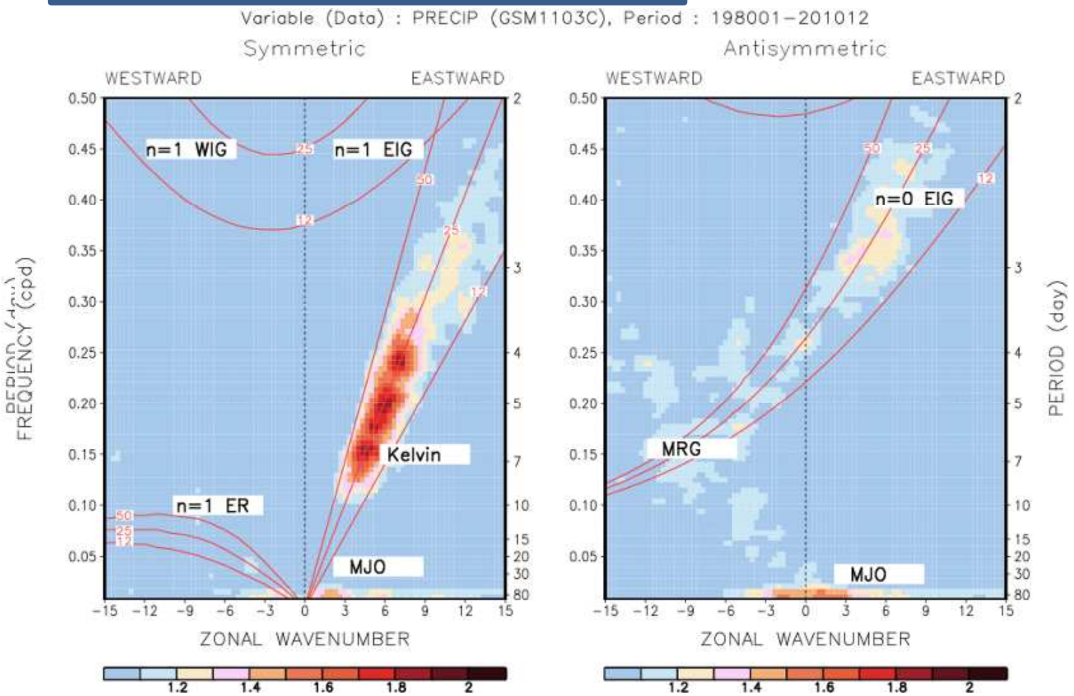

- MJOに対応するスペクトルが再現されていない。
- 赤道ロスビー波も弱い
- ケルビン波の等価深度が観測に比べ「小さい」

熱帯での予測精度 χ200

V1103(ACC)

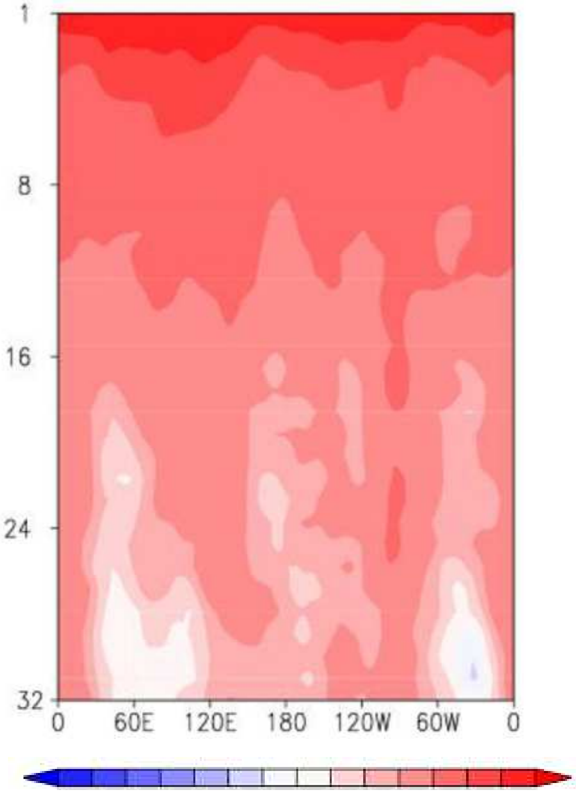

間隔:0,0.1,0.2,0.3,0.5,0.8,0.9

V1103- V0803(ACC)

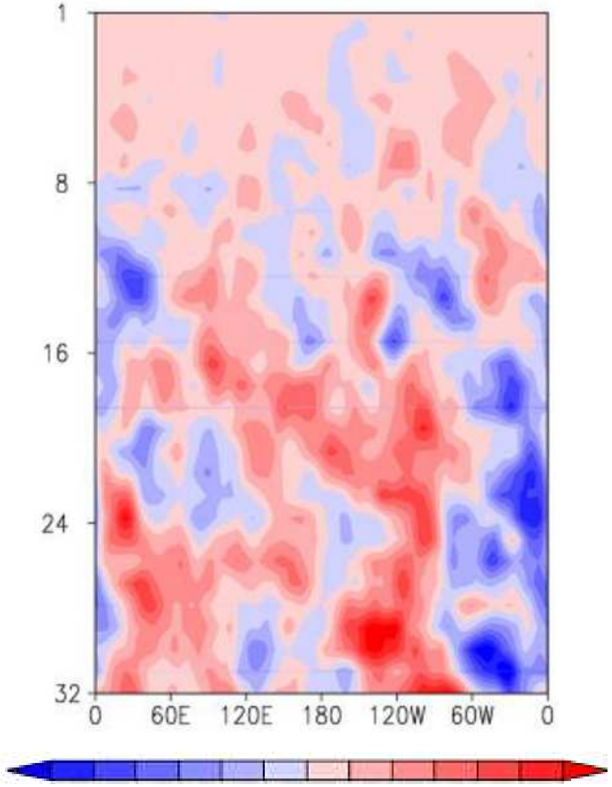

V1103- V0803(RMSE)

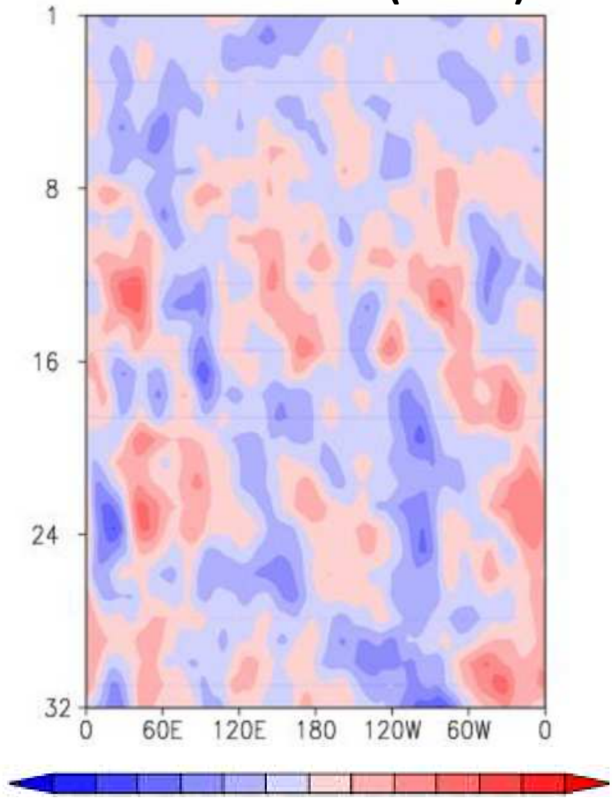

X10^6m^2/s

南北10° 以内を傾度ごとに集計

V1103: 新モデル、熱帯摂動あり
V0803: 旧モデル、熱帯摂動なし

- 熱帯摂動導入後精度が向上。

熱帯での予測精度 χ200

ACC :Phase7-all

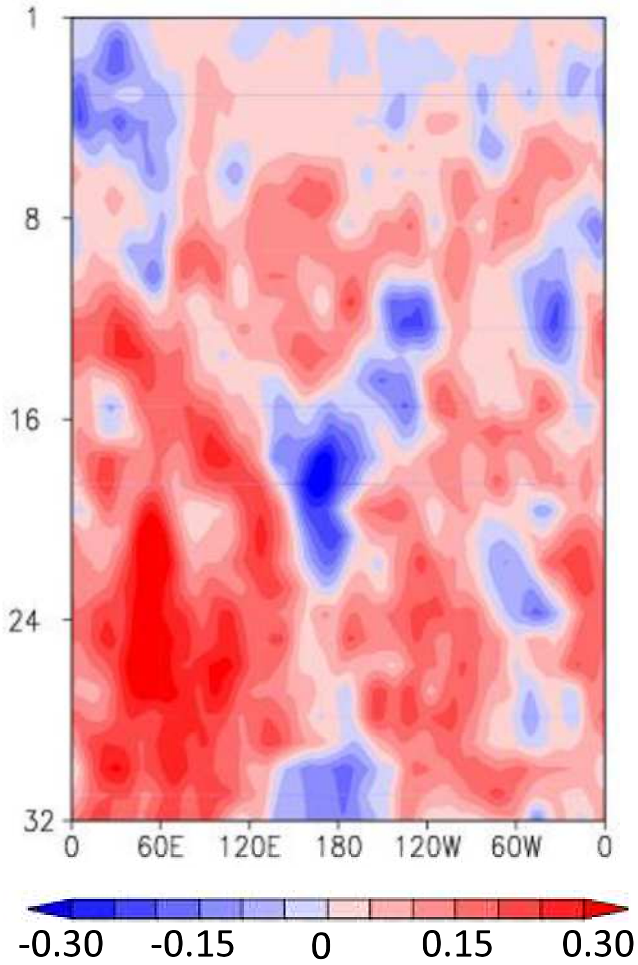

ECMWFモデル(Cy32R)の結果

Phase 6&7
(初期日で太平洋西
部付近で対流活発)

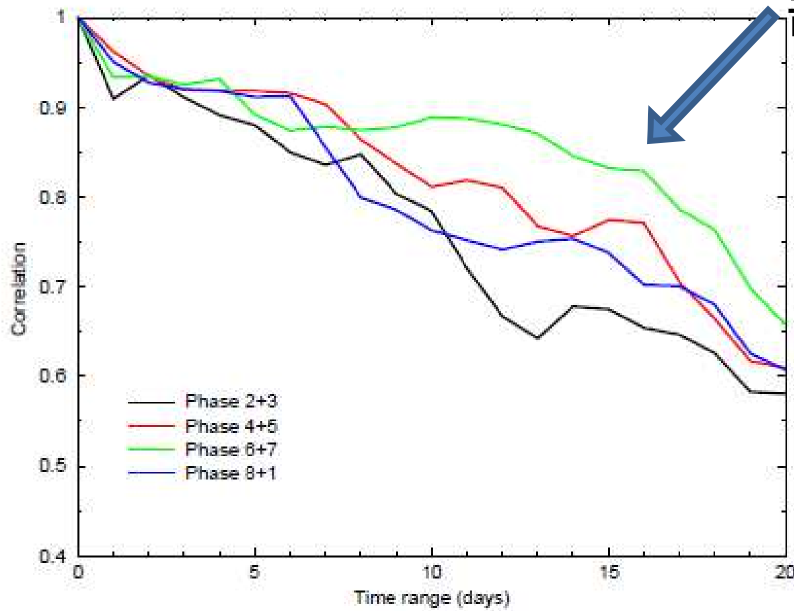

Vitart and Molteni (2009)

- MJOの位相毎に予測精度も異なる。